



# OPTIMAL PLACEMENT OF SOURCES AND SENSORS WITH THE MINIMAX CRITERION FOR ACTIVE CONTROL OF A ONE-DIMENSIONAL SOUND FIELD

P. SERGENT AND D. DUHAMEL

*Ecole Nationale des Ponts et Chaussées. CERAM, 6 et 8, avenue Blaise Pascal,  
Cité Descartes, Champs-sur-Marne, 77455 Marne-La-Vallée Cedex 2, France*

*(Received 23 October 1996, and in final form 16 June 1997)*

The optimization of the placement of secondary sources and error sensors can enhance the efficiency of active noise control. Since the classic quadratic cost functions are not adapted to the search of the optimal placement, it is shown that the “minimax” criterion—minimization of the largest squared pressure at a number of distributed points—better suits the strategy of selection in the placement of sources and sensors. Sufficient numbers of sources and sensors, their locations and the volume velocity of each secondary source are found simultaneously, in a short computation time, by solving a unique linear programming problem. Bounds on the volume velocity are introduced easily. If the number of sources is prescribed, a mixed programming problem is solved. This paper is devoted to the application of this method in a one-dimensional enclosure with rigid walls.

© 1997 Academic Press Limited

## 1. INTRODUCTION

Active noise control consists of reducing an undesirable noise measured at error sensors by adjusting the volume velocity of each secondary source. The attenuation of noise achieved depends on the location of sources and sensors. The optimization of their placement can therefore lead to an additional reduction of noise.

In most of the papers dealing with the optimization of the placement of sources and sensors, the cost function is a quadratic function of the volume velocities. For a single frequency excitation, Curtis [1] presented several quadratic forms and their minimization: the acoustic potential energy, the acoustic intensity, the acoustic power output and the sum of squared pressure at distributed points. These quadratic forms usually have the advantage of representing a physical quantity. Their minimization with respect to the volume velocities is also easy. Unfortunately, their minimization with respect to the locations of sources and sensors is not as easy, since the objective function is not a convex function of the locations and has many local minima. This difficult problem of placement of sources and sensors has been solved by different methods.

These methods usually correspond to two different strategies: selection or gradient minimization. Benzaria and Martin [2] showed that there is a great advantage in combining these two strategies. The strategy of selection consists in defining candidate locations and determining the best placements among them. Natural algorithms such as genetic algorithms and simulated annealing algorithms belong to the strategy of selection. They are promising optimization techniques for the optimal placement of sources and sensors in active noise control [3–5]. They provide near-optimal solutions. Heuristic algorithms are quick and usually iterative methods of selection. All of them, to our knowledge, are

devoted to the placement of secondary sources. Kim and Ih [6] propose two original non-iterative criteria of selection of sources: the sensitivity or the volume velocity of each secondary source when they act together. The iterative heuristic algorithms concern selections by addition [7] or removal [7, 8] if the initial configuration is a single source or a large set of sources.

Once a promising placement of sensors or sources is found, methods of gradient minimization can be applied to improve the quality of the placement. Nayroles *et al.* [9] proposed the use of the diffuse approximation as an interpolation method for experimental data. First, the cost function is minimized with respect to the volume velocities. Second, the gradient algorithm is applied to the optimization of the locations. When the volume velocities are constrained, Yang and Tseng [10] advised optimizing simultaneously the volume velocity and the location of the sources with a gradient-descent algorithm.

Although these previous methods based on a quadratic cost function bring about a large improvement in the search of the optimal placement, they remain unsatisfactory because they just provide near-optimal solutions. In this paper, it is shown that there exists an appropriate cost function that better suits the strategy of selection in the placement of sources and sensors: the largest squared pressure at a number of distributed points. Elliot *et al.* [11] called this cost function the “minimax” criterion. This new cost does not represent an energy like the acoustic potential energy. However, it is useful in many circumstances when the acoustic noise level is compelled by not to exceed a certain level at several points. For the “minimax” criterion, it is shown that an exact solution for the optimal locations of sources and sensors is determined in a very short computation time by solving a unique linear programming problem. Sufficient numbers of sources and sensors, their locations and the volume velocity of each secondary source are found simultaneously. If the number of secondary sources is prescribed, an exact solution for the optimal locations of the secondary sources is determined by solving a mixed programming problem. This paper is devoted to the application of this method to a one-dimensional enclosure with rigid walls.

## 2. OPTIMAL PLACEMENT OF ERROR SENSORS

In this section we present the method of placement of error sensors in a one-dimensional enclosure. After the “minimax criterion” is explained, it is shown that the optimal volume velocities of the sources are found by solving a linear programming problem with a simplex method. It is then proved that there is a sufficient number of error microphones. Their locations are where the modulus of the acoustic pressure is such that, at the other candidate points, the modulus of the pressure is smaller. Finally, the results for a one-dimensional enclosure of length  $L$  with rigid walls are presented for a single or two secondary sources.

### 2.1. THEORETICAL MODEL

Let  $t$  denote the time,  $\omega$  the angular frequency,  $x$  the distance from the left termination,  $j$  the imaginary unit and  $p(x, t)$  the sound pressure. A point monopolar primary source with volume velocity  $q_p(t)$  is located at the left termination (see Figure 1).  $N$  point-monopolar secondary sources are located inside the enclosure. The  $i$ th secondary source with volume velocity  $q_i(t)$  is located at the distance  $x_i$  from the left termination. In a monochromatic sound field, the quantities have a single frequency harmonic time variation and can be represented by the real part of a complex amplitude function multiplied by the harmonic exponential  $e^{-j\omega t}$  such that

$$\begin{aligned} p(x, t) &= \Re(p(x) e^{-j\omega t}), \\ q_p(t) &= \Re(q_p e^{-j\omega t}), \quad q_i(t) = \Re(q_i e^{-j\omega t}), \quad 1 \leq i \leq N. \end{aligned} \quad (1)$$

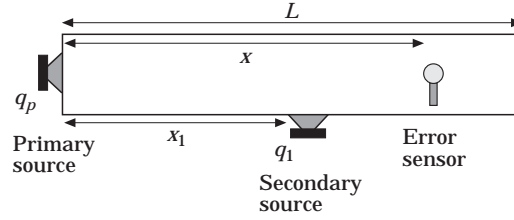


Figure 1. Active noise control system with one secondary source.

Let  $k$  denote the wavenumber equal to  $\omega/c_0$ , where  $c_0$  is the speed of sound. The complex amplitude of the sound pressure  $p(x)$  satisfies the Helmholtz equation and two boundary equations:

$$\frac{d^2 p}{dx^2}(x) + k^2 p(x) = \rho_0 j \omega \sum_{i=1}^N \frac{q_i}{S} \delta_{x_i},$$

$$\frac{dp}{dx}(0) = \rho_0 j \omega \frac{q_p}{S}, \quad \frac{dp}{dx}(L) = 0. \quad (2)$$

Here  $\delta_{x_i}$  is the unidimensional Dirac delta function at point  $x_i$ . The solution of the problem (2) is (see, for example, reference [1])

$$p(x) = \frac{q_p}{S} Z_p(x) + \sum_{i=1}^N \frac{q_i}{S} Z_i(x), \quad Z_p(x) = j \rho_0 c_0 \frac{\cos[k(L-x)]}{\sin(kL)} \quad \forall x,$$

$$Z_i(x) = Z_p(x) \cos(kx_i) \quad \forall x \geq x_i, \quad Z_i(x) = Z_p(x_i) \cos(kx) \quad \forall x \leq x_i. \quad (3)$$

Let the non-dimensional frequency  $\tilde{f}$  be equal to  $kL/\pi$ . The primary and secondary paths then become

$$p(x) = \frac{q_p}{S} Z_p(x) + \sum_{i=1}^N \frac{q_i}{S} Z_i(x),$$

$$Z_p(x) = j \rho_0 c_0 \frac{\cos[\pi \tilde{f}(1-x/L)]}{\sin(\pi \tilde{f})} \quad \forall x,$$

$$Z_i(x) = Z_p(x) \cos(\pi \tilde{f}(x_i/L)) \quad \forall x \geq x_i, \quad Z_i(x) = Z_p(x_i) \cos(\pi \tilde{f}(x/L)) \quad \forall x \leq x_i. \quad (4)$$

Let  $\mathcal{Q}_s$  denote the vector of  $\mathbf{C}^N$  equal to  $(q_1, \dots, q_i, \dots, q_N)$ .

## 2.2. MINIMIZATION

The primary volume velocity is chosen to be equal to 1, for simplicity. The complex sound pressure is now denoted by  $p(x, \mathcal{Q}_s)$ , to indicate the dependence on the secondary volume velocities.

### 2.2.1. Minimax criterion

One can introduce the cost function  $J$ , which is the maximum value of the modulus of the complex pressure ( $J^2$  is the maximum value of the squared pressure) inside a subset

$I$  of the segment  $[0, L]$ . The problem of minimization with respect to the volume velocity  $Q_s$  can be written as

$$\min_{Q_s \in \mathbf{C}^N} J(Q_s) = \max_{x \in I} |p(x, Q_s)|. \quad (5)$$

The minimization of this cost function  $J$  is also called the “minimax” criterion.

### 2.2.2. Enclosure with rigid walls

The fact that the primary and secondary paths are imaginary simplifies the problem of minimization. This is also the case for any three-dimensional enclosure with rigid walls. Instead of searching for a solution in  $\mathbf{C}^N$ , one can show that the problem of minimization is reduced to a problem in  $\mathbf{R}^N$ .

It can be seen easily that

$$|p(x, Q_s)| \geq |p(x, \Re(Q_s))| \quad \forall x \quad \forall Q_s \in \mathbf{C}^N, \quad (6)$$

where  $\Re(Q_s)$  is the vector of  $\mathbf{R}^N$  equal to  $(\Re(q_1), \dots, \Re(q_i), \dots, \Re(q_N))$ . It is deduced that

$$\min_{Q_s \in \mathbf{C}^N} J(Q_s) \geq \min_{\Re(Q_s) \in \mathbf{R}^N} J(\Re(Q_s)). \quad (7)$$

Since  $\mathbf{R}^N \subset \mathbf{C}^N$ ,

$$\min_{Q_s \in \mathbf{C}^N} J(Q_s) \leq \min_{\Re(Q_s) \in \mathbf{R}^N} J(\Re(Q_s)). \quad (8)$$

One concludes that

$$\min_{Q_s \in \mathbf{C}^N} J(Q_s) = \min_{\Re(Q_s) \in \mathbf{R}^N} J(\Re(Q_s)). \quad (9)$$

The problem of minimization is thus reduced to a problem in  $\mathbf{R}^N$ . The primary source and the secondary sources are in phase or in opposition.

### 2.2.3. Linear programming problem

Now consider that the volume velocities  $q_i$  of the secondary sources are real. The vector  $Q_s$  is therefore a vector of  $\mathbf{R}^N$ .

The complex modulus that was used previously can be replaced by an absolute value:

$$(\mathbb{A}) \min_{Q_s \in \mathbf{R}^N} J(Q_s) = \max_{x \in I} |\Im[p(x, Q_s)]|. \quad (10)$$

This problem of minimization can be written as a linear programming problem with  $N + 1$  real variables and  $2 \times \text{card}(I)$  constraint inequalities, where  $\text{card}(I)$  represents the number of points in the subset  $I$ :

$$\min_{Q_s, E} z = E, \quad (11)$$

$$\Im[p(x, Q_s)] \leq \frac{\rho_0 c_0}{S} E \quad \forall x \in I, \quad \Im[p(x, Q_s)] \geq -\frac{\rho_0 c_0}{S} E \quad \forall x \in I. \quad (12)$$

Since the simplex method works provided the variables are of the same sign, the problem is transformed such that all the variables are positive (see Appendix 1).

The solution of a linear programming problem is found at a vertex of the solution space (see the example of Figure 3 of section 2.3.1). A linear programming problem can be reduced to a “combinatorial” problem that consists in determining which  $N + 1$  constraints (out of the  $2 \times \text{card}(I)$  constraint inequalities) are satisfied by the solution. The simplex method, first published by Dantzig [12], finds in an efficient way the optimal

extreme point  $(Q_s^{opt}, E^{opt})$  in the solution space. One can now show that a sufficient number and an optimal placement of error sensors can be deduced from this solution.

### 2.2.3. Sufficient number and placement of error sensors

One can introduce a new cost function  $J'$  and a new problem (B) one has

$$J'(Q_s) = \max_{x \in I'} |\Im[p(x, Q_s)]|, \quad (13)$$

where  $I'$  is the subset of  $I$  such that

$$I' = \left\{ x \in I \mid |\Im[p(x, Q_s^{opt})]| = \frac{\rho_0 c_0}{S} E^{opt} \right\} \quad (14)$$

and hence

$$(B) \min_{Q_s \in \mathbf{R}^N} J'(Q_s). \quad (15)$$

The solution  $(Q_s^{opt}, E^{opt})$  of the problem (A) can be shown to be also a solution of the problem (B) if  $I$  is composed of a finite number of discrete points.

In Appendix 2 it is shown, first, that there exists a ball  $\mathbf{B}$  of  $\mathbf{R}^N$ , centered in  $Q_s^{opt}$ , of radius  $r_0 > 0$  and of boundary  $\delta\mathbf{B}$  such that

$$J(Q_s) = J'(Q_s) \quad \forall Q_s \in \mathbf{B}. \quad (16)$$

In Appendix 3 it is shown, second, that the function  $J'(Q_s)$  is a convex function of  $\mathbf{R}^N$ . If  $Q_0$ ,  $Q_1$  and  $Q_2$  are three points of  $\mathbf{R}^N$  satisfying  $Q_0 = (1-t)Q_1 + tQ_2$ , where  $t$  is a real number in  $]0, 1[$  (the bounds 0 and 1 are excluded), the relation of convexity is

$$J'(Q_0) \leq (1-t)J'(Q_1) + tJ'(Q_2). \quad (17)$$

Equation (16) shows that  $Q_s^{opt}$  is equally a minimum of  $J'(Q_s)$  for  $Q_s \in \mathbf{B}$ :

$$J'(Q_s^{opt}) \leq J'(Q_s) \quad \forall Q_s \in \mathbf{B}. \quad (18)$$

If  $Q_s \in \mathbf{R}^N \setminus \mathbf{B}$ , there exists  $Q_0 \in \delta\mathbf{B}$  and a real number  $t \in ]0, 1[$  such that

$$Q_0 = (1-t)Q_s^{opt} + tQ_s \quad \forall t \in ]0, 1[. \quad (19)$$

Since  $J'(Q)$  is a convex function of  $\mathbf{R}^N$ ,

$$J'(Q_0) \leq (1-t)J'(Q_s^{opt}) + tJ'(Q_s). \quad (20)$$

The inequality (20) gives

$$0 \leq \frac{J'(Q_0) - J'(Q_s^{opt})}{t} \leq J'(Q_s) - J'(Q_s^{opt}). \quad (21)$$

Hence

$$J'(Q_s^{opt}) \leq J'(Q_s) \quad \forall Q_s \in \mathbf{R}^N \setminus \mathbf{B}. \quad (22)$$

With the inequalities (18) and (22) one can conclude that the solution  $(Q_s^{opt}, E^{opt})$  of the problem (A) is also a solution of the problem (B).

This conclusion is very interesting because the same reduction of noise can be achieved by the set  $I$  and by its subset  $I'$ . This means that there is a sufficient number  $M$  of error sensors. This number is equal to  $\text{card}(I')$ . The locations of these error sensors are determined by the subset  $I'$ . In solving the unique linear programming problem (A), the optimal vector of volume velocities  $Q_s^{opt}$  and the sufficient number  $M$  of error sensors and

their locations are determined simultaneously. The  $N + 1$  constraints, which are satisfied at the limit, reveal the microphone locations at which the modulus of the acoustic pressure is such that everywhere else, the modulus is smaller. It does not mean, however, that the better the control is at these locations, the lower the pressure is everywhere else. A fundamental question arises at this stage: As the optimal volume velocity is obtained, what is the use of having microphones? These microphones are indeed theoretically useless. In practical applications, however, they are necessary if an adaptation is performed on-line and has to follow slight variations of the primary signal (change of the location of the primary source or change of the frequency of the signal) and of the environment (change of the temperature). Without any adaptation, the efficiency of the active control can then be largely reduced.

*Remark 1.* If  $I$  contains an infinite number of points the relation (18) must be replaced by a positive directional derivative of  $J$  in  $Q_s^{opt}$ . The convexity of the function  $J$  again assures the final result.

Some additional conclusions on the sufficient number of error sensors can be found if one adds two hypotheses: (i) there is not a perfect cancellation of noise in the zone of silence defined by the set  $I$  (i.e.,  $E^{opt} > 0$ ); (ii) the solution  $(Q_s^{opt}, E^{opt})$  is not degenerate, which means that it corresponds, in the solution space, to the intersection of exactly  $N + 1$  hyperplanes.

With hypotheses (i) and (ii),  $N + 1$  equalities  $\Im[p(x, Q_s^{opt})] = (\rho_0 c_0 / S)E^{opt}$  or  $\Re[p(x, Q_s^{opt})] = -(\rho_0 c_0 / S)E^{opt}$  only are satisfied by the solution. Hence

$$\text{card}(I') = N + 1. \quad (23)$$

The sufficient number  $M$  of error sensors is therefore equal to  $N + 1$  where  $N$  is the number of secondary sources.

*Remark 2.* If hypothesis (ii) is not satisfied, the solution  $(Q_s^{opt}, E^{opt})$  corresponds, in the solution space, to the intersection of more than  $N + 1$  hyperplanes. In this case  $\text{card}(I') > N + 1$ , but some excess points belonging to  $I'$  are useless.

*Remark 3.* If hypothesis (i) is not satisfied, there is a perfect cancellation of noise. An additional equality is satisfied (i.e.,  $E^{opt} = 0$ ) by the solution so that equation (23) is replaced by

$$\text{card}(I') + 1 = N + 1. \quad (24)$$

The sufficient number  $M$  of error sensors is therefore equal to  $N$  in this special case.

### 2.3. APPLICATION WITH ONE SOURCE

To be presented here is an application of the method with one secondary source. The advantage of using a single secondary source is that the solution space is a convex space of  $\mathbf{R} \times \mathbf{R}^+$  that can be drawn easily ( $\mathbf{R}^+$  is the set of the positive real numbers). If there is an infinity of points in an interval, the solution space is bounded by an envelope of straight lines that makes up a caustic. An example is chosen where the non-dimensional frequency  $\tilde{f}$  is equal to  $1/2$  and the location of the secondary source is equal to  $L/2$ . Five different subsets  $I$  of the segment  $[0, L]$  are chosen.

#### 2.3.1. Subset $I$ equal to $\{0.25, 0.5, 1.0\}$

The subset  $I$ , on which the cost function  $J$  is defined, contains three points denoted as  $M_1$ ,  $M_2$  and  $M_3$  the co-ordinates of which are equal to  $0.25$ ,  $0.50$  and  $1.00$  respectively (see Figure 2). The linear programming problem (11), (12) now contains six inequalities from which the solution space of this simple problem is built. The sound pressure  $p(x, q_1)$  is deduced from equations (4):

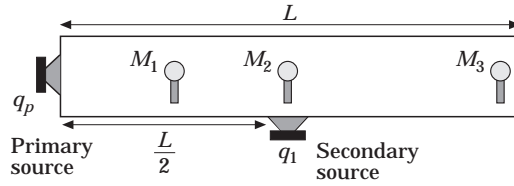


Figure 2. Locations of error sensors with  $I = \{0.25, 0.5, 1\}$ .

$$\min_{q_1, E} z = E, \tag{25}$$

$$\left\{ \begin{array}{l} \sin(\pi/8) + q_1(\sqrt{2}/2) \cos(\pi/8) \leq E \\ (\sqrt{2}/2) + q_1 \cdot 1/2 \leq E \\ 1 + q_1 \sqrt{2}/2 \leq E \\ \sin(\pi/8) + q_1(\sqrt{2}/2) \cos(\pi/8) \geq -E \\ \sqrt{2}/2 + q_1 \cdot 1/2 \geq -E \\ 1 + q_1 \sqrt{2}/2 \geq -E \end{array} \right. \tag{26}$$

This solution space is presented in Figure 3. The solution  $(q_1^{opt}, E^{opt})$  of the linear programming problem is found in this figure and is equal to

$$\left( -\sqrt{2} \frac{1 + \sin(\pi/8)}{1 + \cos(\pi/8)}, \frac{\cos(\pi/8) - \sin(\pi/8)}{1 + \cos(\pi/8)} \right).$$

What is more interesting is that, among the six inequalities, only two are satisfied at the limit and determine the solution  $q_1^{opt}$ :

$$\left\{ \begin{array}{l} 1 + q_1^{opt} \sqrt{2}/2 = E^{opt} \\ \sin(\pi/8) + q_1^{opt} (\sqrt{2}/2) \cos(\pi/8) = -E^{opt} \end{array} \right. \tag{27}$$

These two inequalities correspond to the points  $M_1$  and  $M_3$ . That means that the point  $M_2$ , in this problem, is useless. The same solution  $q_1^{opt}$  would have been found for the “minimax” criterion with the points  $M_1$  and  $M_3$  only.

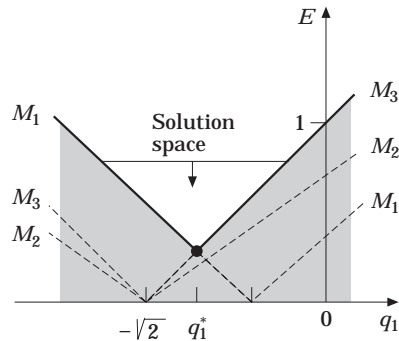


Figure 3. Solution space of the linear programming with  $I = \{0.25, 0.5, 1\}$ .

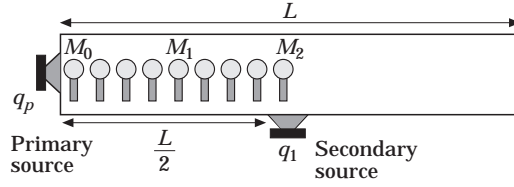


Figure 4. Locations of error sensors with  $I = [0, L/2]$ .

This simple problem shows that, in solving a unique linear programming problem, the optimal volume velocity  $q_1^{opt}$ , a sufficient number (equal to two) of error sensors and their locations (locations  $M_1$  and  $M_3$ ) are determined simultaneously.

2.3.2. *Subset I equal to  $[0, L/2]$*

Instead of dealing with a discrete subset  $I$ , consider now that this subset contains an infinite number of points and is equal to  $[0, L/2]$  (see Figure 4). As previously, one can build the solution space shown in Figure 5 and determine the solution  $(q_1^{opt}, E^{opt})$ . This solution is equal to  $(-\sqrt{2}/(1 + \sqrt{2}), 1/(1 + \sqrt{2}))$ . The construction of the solution space is explained in detail in section 2.3.4. Among the infinite set of inequalities, two only are satisfied at the limit by the solution:

$$\begin{aligned} \sqrt{2}/2 + q_1^{opt}1/2 &= E^{opt} \\ q_1^{opt}\sqrt{2}/2 &= -E^{opt} \end{aligned} \quad (28)$$

They correspond to the points  $M_0$  and  $M_2$ . This example shows that the sufficient number of error sensors is again equal to two. The optimal points are determined here from an infinite set of candidate locations.

2.3.3. *Subset I equal to  $[L/2, L]$*

Now consider that the whole subset  $I$  is located on the right side of the secondary source. In the example the subset  $I$  is equal to the segment  $[L/2, L]$  (see Figure 6). As previously, one can build the solution space shown in Figure 7 (see section 2.3.4 for details) and determine the solution  $(q_1^{opt}, E^{opt})$ . This solution is equal to  $(-\sqrt{2}, 0)$ . This case is singular because hypotheses (i) and (ii) of section 2.2 are not satisfied. There is a perfect cancellation of the noise at each point of the subset  $I$ . The solution is also degenerate. The sufficient number of error sensors is equal to 1 and each location is optimal. This result is well known

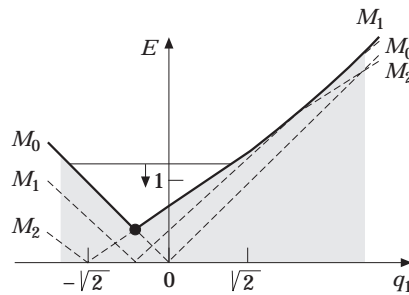


Figure 5. The solution space of the linear programming with  $I = [0, L/2]$ .



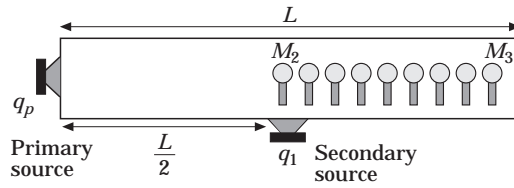


Figure 6. Locations of error sensors with  $I = [L/2, L]$ .

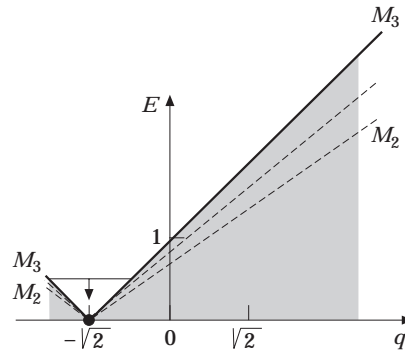


Figure 7. The solution space of the linear programming with  $I = [L/2, L]$ .

for the active noise control of a sound wave: a secondary source can cancel the noise downstream and all the locations of error sensors are equivalent.

2.3.4. *Subset I equal to [0, L]*

The zone of silence now represents the whole enclosure (see Figure 8). This case is interesting because the conclusions can be compared with the work of Curtis [1] and of Nelson and Elliott [13], who used the acoustic potential energy in the enclosure as the cost function. As previously, one can build the solution space shown in Figure 9 and determine the solution  $(q_1^{opt}, E^{opt})$ . This solution is equal to  $(-\sqrt{2}/2, 1/2)$ . Among the infinite set of inequalities, two only are satisfied by the solution:

$$\begin{aligned} 1 + q_1^{opt} \sqrt{2}/2 &= E^{opt} \\ q_1^{opt} \sqrt{2}/2 &= -E^{opt} \end{aligned} \quad (29)$$

They correspond to the points  $M_0$  and  $M_3$  (i.e., the two terminations of the enclosure). This particular placement of error sensors is actually optimal for a broad range of frequencies depending on the location  $x_1$  of the secondary source with respect to the wavelength  $\lambda$  of the signal. One can separate the problem of placement into two cases

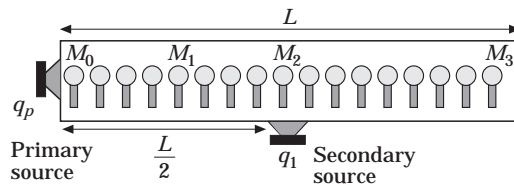


Figure 8. Locations of error sensors with  $I = [0, L]$ .

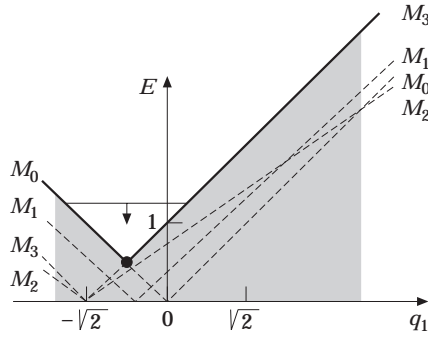


Figure 9. The solution space of the linear programming with  $I = [0, L]$ .

according to whether the distance  $x_1$  is inferior or superior to the quarter wavelength of the signal. First one can determine the solution space for any frequency.

2.3.4.1. Construction of the solution space  $S$ . The solution space  $S$  is defined as a convex space of  $\mathbf{R} \times \mathbf{R}^+$  equal to  $S_1 \cap S_2$  such that

$$S_1 = \left\{ (q_1, E) \in \mathbf{R} \times \mathbf{R}^+ \mid |\Im[p(x, q_1)]| \leq \frac{\rho_0 c_0}{S} E \quad \forall x \in [x_1, L] \right\},$$

$$S_2 = \left\{ (q_1, E) \in \mathbf{R} \times \mathbf{R}^+ \mid |\Im[p(x, q_1)]| \leq \frac{\rho_0 c_0}{S} E \quad \forall x \in [0, x_1] \right\}, \quad (30)$$

Since  $|\Im[p(x, q_1)]| \leq |\Im[p(L, q_1)]|$  for all  $x$  in  $[x_1, L]$

$$S_1 = \{(q_1, E) \in \mathbf{R} \times \mathbf{R}^+ \mid |\Im[p(L, q_1)]| \leq (\rho_0 c_0 / S) E\}. \quad (31)$$

The space  $S_1$  is therefore bounded by two straight lines that are defined by  $M_3$ , and that one can call  $\mathbb{D}_3^-$  and  $\mathbb{D}_3^+$ :

$$\mathbb{D}_3 \left\{ \begin{array}{l} \Im[p(L, q_1)] = (\rho_0 c_0 / S) E \quad \mathbb{D}_3^+ \\ \Im[p(L, q_1)] = -(\rho_0 c_0 / S) E \quad \mathbb{D}_3^- \end{array} \right\}. \quad (32)$$

The space  $S_2$  is the intersection of two spaces  $S_2^-$  and  $S_2^+$  of  $\mathbf{R} \times \mathbf{R}^+$  such that

$$S_2^+ = \{(q_1, E) \in \mathbf{R} \times \mathbf{R}^+ \mid \Im[p(x, q_1)] \leq (\rho_0 c_0 / S) E \quad \forall x \in [0, x_1]\},$$

$$S_2^- = \{(q_1, E) \in \mathbf{R} \times \mathbf{R}^+ \mid -\Im[p(x, q_1)] \leq (\rho_0 c_0 / S) E \quad \forall x \in [0, x_1]\}. \quad (33)$$

Each space  $S_2^+$  and  $S_2^-$  is bounded by an envelope of straight lines that are denoted by  $\mathbb{D}^+(x)$  and  $\mathbb{D}^-(x)$  respectively with  $x \in [0, x_1]$ :

$$\Im[p(x, q_1)] = (\rho_0 c_0 / S) E \quad \mathbb{D}^+(x)$$

$$\Im[p(x, q_1)] = -(\rho_0 c_0 / S) E \quad \mathbb{D}^-(x) \quad (34)$$

The envelopes of straight lines are defined as the tangents of two curves  $\mathbb{C}^+$  and  $\mathbb{C}^-$ . The curve  $\mathbb{C}^+$  contains the intersection of the straight lines  $\mathbb{D}^+(x + \Delta x)$  and  $\mathbb{D}^+(x)$  when

$x$  varies and when  $\Delta x$  tends to zero. The parametric equations  $(E(x), q_1(x))$  satisfied by the curve  $\mathbb{C}^+$  are determined from the equations

$$\left\{ \begin{array}{l} \mathfrak{I}[p(x, q_1)] = \frac{\rho_0 c_0}{S} E \quad \mathbb{D}^+(x) \\ \mathfrak{I}[p(x, q_1)] + \mathfrak{I}\left[\frac{\partial p}{\partial x}(x, q_1(x))\right] \Delta x = \frac{\rho_0 c_0}{S} E \quad \mathbb{D}^+(x + \Delta x) \end{array} \right\}. \quad (35)$$

Subtracting and adding these two last equations yields

$$\mathfrak{I}\left[\frac{\partial p}{\partial x}(x, q_1(x))\right] = 0, \quad \mathfrak{I}[p(x, q_1(x))] = \frac{\rho_0 c_0}{S} E(x). \quad (36)$$

One deduces that

$$\mathbb{C}^+ \left\{ \begin{array}{l} E(x) = \frac{1}{\sin(\pi\tilde{f}(x/L))} \\ q_1(x) = \frac{\sin(\pi\tilde{f}(1-x/L))}{\cos(\pi\tilde{f}(1-x_1/L)) \sin(\pi\tilde{f}(x/L))} \end{array} \right. \quad x \in [0, x_1]. \quad (37)$$

The curve  $\mathbb{C}^-$  is the symmetric curve of  $\mathbb{C}^+$  with respect to the straight line  $E = 0$ . The curve  $\mathbb{C}^+$  belongs to the hyperbolic curve  $\mathbb{H}$  the Cartesian equation of which is

$$E^2 = 1 + \left( \frac{\cos(\pi\tilde{f}) + q_1 \cos(\pi\tilde{f}(1-x_1/L))}{\sin(\pi\tilde{f})} \right)^2. \quad (38)$$

The straight lines  $\mathbb{D}^+(0)$  and  $\mathbb{D}^-(0)$  are the asymptotes of the hyperbolic curve  $\mathbb{H}$ . The solution space  $S$  is finally bounded by the straight lines  $\mathbb{D}_3^+$  and  $\mathbb{D}_3^-$ , and by the tangents of the curves  $\mathbb{C}^+$  and  $\mathbb{C}^-$ .

2.3.4.2. The distance  $x_1$  is inferior to  $\lambda/4$ . When the distance  $x_1$  is inferior to  $\lambda/4$ , one can show that the optimal placement for the sensors is the couple  $M_0, M_3$ .

When  $x$  varies from 0 to  $x_1$ , the corresponding point of  $\mathbb{C}^+$  goes from one end of  $\mathbb{H}$  to the point  $(E(x_1), q_1(x_1))$ . When the distance  $x_1$  is inferior to  $\lambda/4$ ,  $E(x) > 1$  for all  $x$  in  $[0, x_1]$ . The curve  $\mathbb{C}^+$  is included in one quarter of the hyperbolic curve  $\mathbb{H}$  (see Figure 10) and does not contain the top of  $\mathbb{H}$  the co-ordinates of which are  $(-\cos(\pi\tilde{f})/\cos[\pi\tilde{f}(1-x_1/L)], 1)$ . The construction of the boundary of  $S$ , explained in (section 2.3.4.1.), gives a solution space bounded by the straight lines  $\mathbb{D}_3^+, \mathbb{D}_3^-, \mathbb{D}^-(0)$  and  $\mathbb{C}^+$ . The optimal solution  $(q_1^{opt}, E^{opt})$  belongs to  $\mathbb{D}_3 \cap \mathbb{D}^-(0)$ . The optimal placement for sensors is then the couple  $M_0, M_3$ .

When the distance  $x_1$  is equal to  $\lambda/4$ , the pressure at the right side of the secondary source is independent of the volume velocity  $q_1$ . The curve  $\mathbb{C}^+$  corresponds exactly to one quarter of the hyperbolic curve  $\mathbb{H}$ . The solution space contains two optimal extreme points (see Figure 11) that belong to  $\mathbb{D}_3 \cap \mathbb{D}^-(0)$  and  $\mathbb{D}_3 \cap \mathbb{C}^+$  respectively.

2.3.4.3. The distance  $x_1$  is superior to  $\lambda/4$ . When  $\lambda/4 < x_1 < \lambda/2$ , the curve  $\mathbb{C}^+$  contains one quarter of the hyperbolic curve  $\mathbb{H}$  and a top of  $\mathbb{H}$ . The construction of the boundary of  $S$  explained in (section 2.3.4.1.) gives a solution space bounded again by the straight lines  $\mathbb{D}_3^+, \mathbb{D}_3^-, \mathbb{D}^-(0)$  and  $\mathbb{C}^+$ . However, the optimal point no longer belongs to  $\mathbb{D}_3 \cap \mathbb{D}^-(0)$ .

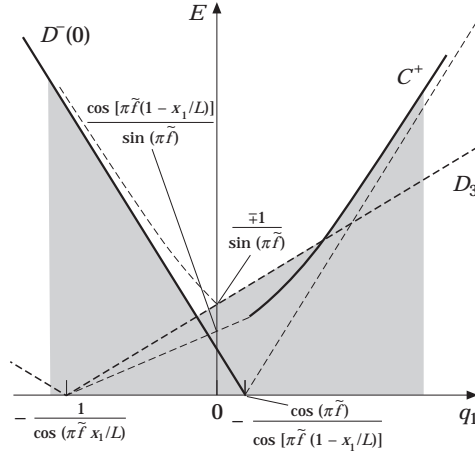


Figure 10. The solution space of the linear programming with  $I = [0, L]$  and  $x_1 < \lambda/4$ .

When the distance  $x_1$  is superior to  $\lambda/2$  the curve  $\mathbb{C}^+$  contains one half of the hyperbolic curve  $\mathbb{H}$ . The solution space is bounded by the straight lines  $\mathbb{D}_3^+$ ,  $\mathbb{D}_3^-$  and  $\mathbb{C}^+$  only.

In this domain of frequencies, the solution of the problem of placement depends on frequency and two kinds of solution can be distinguished, as follows.

A. The solution belongs to  $\mathbb{D}_3 \cap \mathbb{C}^+$  (see Figure 12). In this case the optimal placement for the error sensors is the point  $M_3$  at the right termination and a point belonging to the segment  $[0, x_1]$ .

B. The solution is at the top of the hyperbolic curve  $\mathbb{H}$  (see Figure 13). The corresponding point of  $[0, x_1]$  is denoted  $x_0$ . The secondary acoustic path  $Z_1(x_0)$  is zero at this point such that

$$\cos(\pi \tilde{f}(x_0/L)) = 0. \tag{39}$$

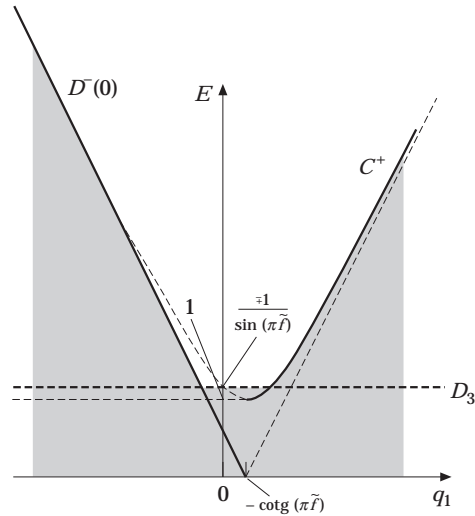


Figure 11. The solution space of the linear programming with  $I = [0, L]$  and  $x_1 = \lambda/4$ .

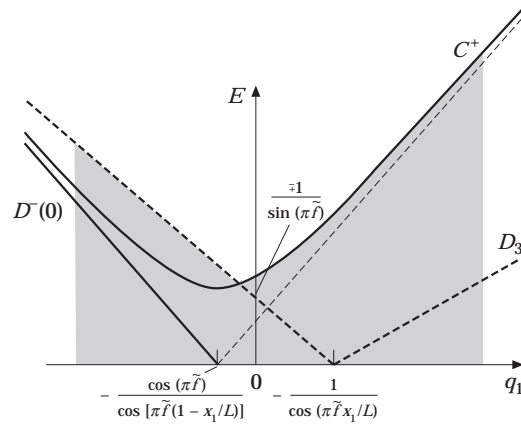


Figure 12. The solution space of the linear programming with  $I = [0, L]$  and  $x_1 > \lambda/4$ .

It can be verified that one point  $x_0$  at least exists, since  $x_1 > \lambda/4$ :

$$\pi\tilde{f}(x_1/L) > \pi/2 > 0. \tag{40}$$

There then exists at least one point  $x_0$  in  $[0, x_1]$  such that

$$\pi\tilde{f}(x_0/L) = \pi/2. \tag{41}$$

This point  $x_0$  satisfies equation (39). The optimal placement for two error sensors corresponds, in this case, to a pair of sensors located at the points  $x_0$  and  $x_0 + \Delta x$ , where  $\Delta x$  is small. The result of the control leads to

$$p(x_0, q_1^{opt}) = p(x_0 + \Delta x, q_1^{opt}) = j(\rho_0 c_0 / S)E^{opt}. \tag{42}$$

When  $\Delta x$  tends to zero, the optimal volume velocity satisfies

$$\frac{\partial p}{\partial x}(x_0, q_1^{opt}) = 0. \tag{43}$$

This result can be achieved by the measurement of the acoustic particle velocity at the point  $x_0$  and by the minimization of the kinetic energy at this point.

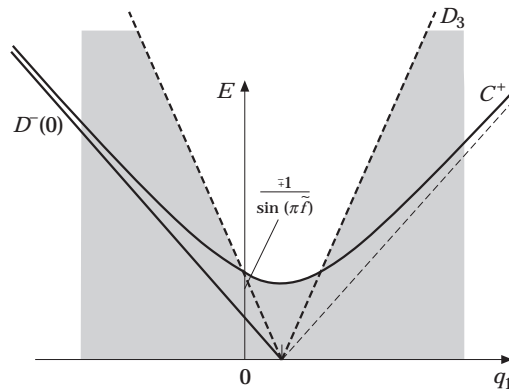


Figure 13. The solution space of the linear programming with  $I = [0, L]$  and  $x_1 > \lambda/4$ .

The sound pressure  $p(x_0, q_1)$  at this point cannot be modified by an active control since the secondary acoustic path  $Z_1(x_0)$  is zero:

$$|\mathfrak{J}[p(x_0, q_1)]| = \frac{\rho_0 c_0}{S} \left| \frac{\cos[\pi\tilde{f}(1 - x_0/L)]}{\sin(\pi\tilde{f})} \right| = \frac{\rho_0 c_0}{S}. \quad (44)$$

Equation (44) shows that, when the distance  $x_1$  is superior to  $\lambda/4$ ,  $J(q_1)$  is lower bounded by  $\rho_0 c_0/S$  for all volume velocity  $q_1$ . One can conclude that

$$E^{opt} \geq 1. \quad (45)$$

The cost function  $J(0)$  without control is equal to  $\rho_0 c_0/S \sin(\pi\tilde{f})$  such that

$$1 \leq E^{opt} \leq 1/\sin(\pi\tilde{f}). \quad (46)$$

The inequalities (46) show that  $E = 1$  before and after control around the antiresonance frequencies when  $x_1$  is superior to  $\lambda/4$ . The control therefore has no effect around the antiresonance frequencies when  $x_1$  is superior to  $\lambda/4$ . This result is similar to the considerations of Nelson and Elliott [13], who explained that, between the resonances of the enclosure, there are many modes contributing to the acoustic potential energy, and that the secondary source cannot control any one of these without significantly exciting the others.

### 2.3.5. Subset $I$ equal to $\{0, L/100, \dots, i \times L/100, \dots, 99 \times L/100, L\}$

Numerical applications usually require one to discretize the set  $I$  that represents the zone of silence. The subset  $I$  of section 2.3.4. is now discretized and contains a regular mesh of 101 points ranging from 0 to  $L$  with a step equal to  $L/100$ .

Consider locations of the secondary source equal to  $L/2$  or  $L/3$ . Curtis [1] noticed that the latter location gives good reduction in acoustic potential energy over a range of frequencies.

The simplex method is used to solve this linear programming problem. Results of placement of sensors are presented in Table 1. The results confirm the conclusions of section 2.3.4. When the distance  $x_1$  is inferior to  $\lambda/4$ , the optimal placement for sensors is at the terminations of the enclosure. For smaller wavelengths, two kinds of placement are found: the point  $M_3$  associated with a point of the segment  $[0, x_1]$  or a pair of sensors on a node of the secondary path.

In Figure 14, the maximal modulus of the non-dimensional sound pressure  $E$  in the enclosure is presented when  $x_1$  is equal to  $L/3$ . The sound pressure is visualized first without active control, then with active control and optimally located sensors at each frequency, at last with active control and sensors located at the terminations of the enclosure (i.e., points  $M_0, M_3$ ). When the two sensors are optimally located, it was demonstrated in section 2.2 that the active control is as efficient as an active control with an infinite number of sensors (represented here by 101 sensors). That is why the active control always leads to a reduction of the global cost function. With the two sensors  $M_0, M_3$ , it is found again that this placement is optimal for frequencies inferior to 1.5. The frequency  $\tilde{f} = 1.5$  corresponds to a wavelength equal to  $4x_1$ . For frequencies superior to 1.5, this placement is no longer optimal, but remains a ‘good’ placement. It must be noticed that the active control can, however, lead to an increase of the cost function when the sensors are not optimally located.

Figure 15 represents the same calculations as the previous figure except that  $x_1$  is now equal to  $L/2$ . The placement  $M_0, M_3$  for the two sensors is now optimal for frequencies inferior to 1.0. As already mentioned by Curtis [1], the middle of the enclosure is not a

TABLE 1  
Optimal locations of error sensors  $X_1$  and  $X_2$  divided by  $L$

$\tilde{f}$	$x_1$	
	$L/2$	$L/3$
0.1	0.0 1.0	0.0 1.0
0.2	0.0 1.0	0.0 1.0
0.3	0.0 1.0	0.0 1.0
0.4	0.0 1.0	0.0 1.0
0.5	0.0 1.0	0.0 1.0
0.6	0.0 1.0	0.0 1.0
0.7	0.0 1.0	0.0 1.0
0.8	0.0 1.0	0.0 1.0
0.9	0.0 1.0	0.0 1.0
1.0	0.0 1.0	0.0 1.0
1.1	0.09 1.0	0.0 1.0
1.2	0.17 1.0	0.0 1.0
1.3	0.23 1.0	0.0 1.0
1.4	0.29 1.0	0.0 1.0
1.5	0.33 1.0	0.0 1.0
1.6	0.31 0.32	0.29 1.0
1.7	0.29 0.30	0.25 1.0
1.8	0.27 0.28	0.22 1.0
1.9	0.26 0.27	0.19 1.0

good placement for the secondary source, whereas  $x_1 = L/3$  is rather good. Moreover, these results confirm that the non-dimensional sound pressure  $E$  is superior to 1 when the distance  $x_1$  is superior to one quarter of the wavelength.

#### 2.4. RETURN TO A QUADRATIC COST

Once the two optimal locations  $X_1$  and  $X_2$  for error sensors are known, one can show that the active control that determines the volume velocity  $q_1^{opt}$  can be written as a “minimax” problem (B) or a quadratic problem (B’).

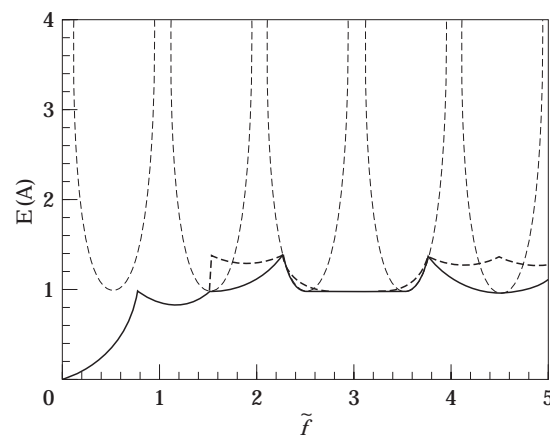


Figure 14. The maximal modulus of the non-dimensional sound pressure: primary (—), controlled with optimally located sensors (---) and controlled with two sensors, the locations  $X_1$  and  $X_2$  of which are 0 and  $L$  (-.-). The location  $x_1$  of the secondary source is  $L/3$ .

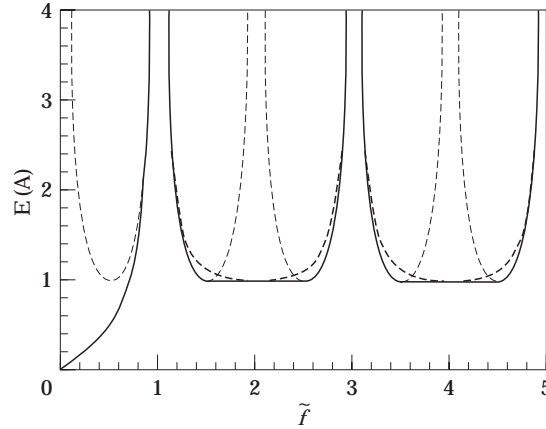


Figure 15. As in Figure 14, except that the location of the secondary source is  $L/2$ .

First recall the expression for the problem (B) when there is a single secondary source:

$$(B) \min_{q_1 \in \mathbf{R}} J'(q_1) = \max(|\Im[p(X_1, q_1)]|, |\Im[p(X_2, q_1)]|). \quad (47)$$

Since the optimal volume velocity  $q_1^{opt}$  satisfies  $|\Im[p(X_1, q_1^{opt})]| = |\Im[p(X_2, q_1^{opt})]|$ , it is also a solution of the problem (B') such that

$$(B') \left\{ \begin{array}{l} \min_{q_1 \in \mathbf{R}} J''(q_1) = \Im^2[p(X_1, q_1)] + \Im^2[p(X_2, q_1)] \\ \Im^2[p(X_1, q_1)] - \Im^2[p(X_2, q_1)] = 0 \end{array} \right\}. \quad (48)$$

Upon using a Lagrange multiplier  $h$ , the volume velocity  $q_1^{opt}$  is now an extremum of the augmented function  $\tilde{J}''$ :

$$\tilde{J}''(q_1) = \Im^2[p(X_1, q_1)] + \Im^2[p(X_2, q_1)] + h\{\Im^2[p(X_1, q_1)] - \Im^2[p(X_2, q_1)]\}. \quad (49)$$

One can now show that  $-1 \leq h \leq 1$  and that  $q_1^{opt}$  is a minimum of  $\tilde{J}''$ .

One introduces the volume velocities  $q_\alpha$  and  $q_\beta$  such that

$$\Im[p(X_1, q_\alpha)] = \Im[p(X_2, q_\alpha)], \quad \Im[p(X_1, q_\beta)] = -\Im[p(X_2, q_\beta)]. \quad (50)$$

The optimal volume velocity  $q_1^{opt}$  is equal to  $q_\alpha$  if  $|\Im[p(X_1, q_\alpha)]| \leq |\Im[p(X_1, q_\beta)]|$  and to  $q_\beta$  elsewhere:

$$\begin{aligned} q_\alpha &= -\frac{Z_p(X_2) - Z_p(X_1)}{Z_1(X_2) - Z_1(X_1)}, & q_\beta &= -\frac{Z_p(X_2) + Z_p(X_1)}{Z_1(X_2) + Z_1(X_1)}, \\ |\Im[p(X_1, q_\alpha)]| &= \left| \frac{Z_1(X_2)Z_p(X_1) - Z_p(X_2)Z_1(X_1)}{Z_1(X_2) - Z_1(X_1)} \right|, \\ |\Im[p(X_1, q_\beta)]| &= \left| \frac{Z_1(X_2)Z_p(X_1) - Z_p(X_2)Z_1(X_1)}{Z_1(X_2) + Z_1(X_1)} \right|. \end{aligned} \quad (51)$$

Hence

$$q_1^{opt} = q_\alpha \quad \text{if } Z_1(X_2)Z_1(X_1) \leq 0, \quad q_1^{opt} = q_\beta \quad \text{if } Z_1(X_2)Z_1(X_1) \geq 0. \quad (52)$$



Since  $q_1^{opt}$  is an extremum of the augmented function  $\tilde{J}''$ , it satisfies the equation

$$(1+h)Z_1(X_1)\Im[p(X_1, q_1^{opt})] + (1-h)Z_1(X_2)\Im[p(X_2, q_1^{opt})] = 0. \quad (53)$$

Equations (52) and (53) finally give the expression for the Lagrange multiplier:

$$h = -\frac{Z_1(X_1) + Z_1(X_2)}{Z_1(X_1) - Z_1(X_2)} \quad \text{if } Z_1(X_2)Z_1(X_1) \leq 0,$$

$$h = -\frac{Z_1(X_1) - Z_1(X_2)}{Z_1(X_1) + Z_1(X_2)} \quad \text{if } Z_1(X_2)Z_1(X_1) \geq 0. \quad (54)$$

One can verify first that  $-1 \leq h \leq 1$  and rewrite the cost function  $\tilde{J}''$ :

$$\tilde{J}''(q_1) = (1+h)\Im^2[p(X_1, q_1)] + (1-h)\Im^2[p(X_2, q_1)]. \quad (55)$$

The cost function  $J''$  is a quadratic form and  $q_1^{opt}$  is a minimum.

Two borderline cases can be pointed out.

The Lagrange multiplier  $h$  is zero when the moduli of the secondary paths  $|Z_1(X_1)|$  and  $|Z_1(X_2)|$  are identical. The problem of minimization then consists of applying a classic quadratic control: the sum of the squared pressures.

When one of the two error sensors is on a node of the secondary acoustic path, the absolute value of the Lagrange multiplier  $|h|$  is one.

The value of the Lagrange multiplier for two different locations of the secondary source is presented in Table 2. It is pointed out that the location of the secondary source in the middle of the enclosure is particular in so far as the Lagrange multiplier is zero when the two error sensors are at the two terminations. The use of  $\tilde{J}''$  can be useful for practical applications. The problem (B') can be solved indeed by classic control algorithms.

TABLE 2

*The Lagrange multiplier  $h$  for two different locations  $x_1$  of the secondary source*

$\tilde{f}$	$x_1$	
	$L/2$	$L/3$
0.1	0.0	0.01
0.2	0.0	0.03
0.3	0.0	0.08
0.4	0.0	0.15
0.5	0.0	0.27
0.6	0.0	0.45
0.7	0.0	0.75
0.8	0.0	0.73
0.9	0.0	0.31
1.0	0.0	0.0
1.1	0.02	-0.24
1.2	0.11	-0.45
1.3	0.26	-0.63
1.4	0.55	-0.81
1.5	0.97	-1.0
1.6	0.50	-0.03
1.7	0.18	-0.01
1.8	-0.56	0.09
1.9	0.37	0.18

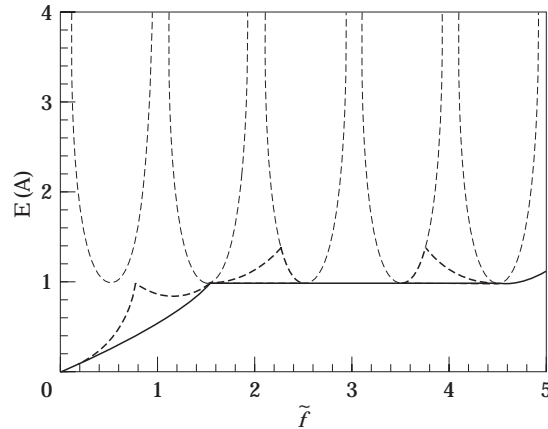


Figure 16. The maximal modulus of the non-dimensional sound pressure: primary (---), controlled with optimally located sensors by two secondary sources  $x_1 = L/3$  and  $x_2 = L/2$  (—) and controlled by one secondary source  $x_1 = L/3$  (-.-).

### 2.5. APPLICATION WITH TWO SOURCES

When two secondary sources are used, the sufficient number of error sensors is equal to three.

Suppose that one chooses two secondary sources with respective locations  $x_1$  and  $x_2$  equal to  $L/3$  and  $L/2$  and a zone of silence described by the set  $I$  of section 2.3.5.

When the distance  $x_1$  of the closest secondary source is inferior to the quarter of the wavelength, a significant attenuation is again achieved (see Figure 16). The optimal placement of the error sensors now depends on frequency and the locations are summed up in Table 3.

When the distance  $x_1$  of the closest secondary source is superior to the quarter of the wavelength, the conclusion of section 2.3, saying that  $E^{opt} \geq 1$ , is still valid. In the band of frequencies  $[1.5, 5.0]$ , this bound is reached for almost all the frequencies with an active control by two secondary sources. At many frequencies, the second source is even useless so that the sufficient numbers of sources and sensors are often reduced to 1 and 2 respectively.

### 3. OPTIMAL PLACEMENT OF SECONDARY SOURCES

This section is devoted to the optimal placement of secondary sources in a unidimensional enclosure with rigid walls of length  $L$ . The primary volume velocity is chosen equal to 1. The secondary volume velocities can then be chosen real following remark 2.2.1.

TABLE 3  
*Optimal locations of the three sufficient error sensors*

Frequencies	Optimal locations		
[0.00–0.67]	0.0	0.33	0.34
[0.68–1.27]	0.0	0.33	1.00
[1.28–1.50]	0.0	0.33	0.34

## 3.1. A SINGLE SECONDARY SOURCE

One wants to determine the influence of the location  $x_1$  of a single secondary source on the “minimax” criterion defined in section 2.2. The zone of silence represents the whole enclosure so that  $I = [0, L]$ .

3.1.1. *The distance  $x_1$  is inferior to the quarter of the wavelength*

When the distance  $x_1$  is inferior to the quarter of the wavelength, one can determine the maximal modulus  $E^{opt}$  of the non-dimensional sound pressure inside the zone of silence and present its variations with respect to the location  $x_1$  of the secondary source.

One knows indeed, from section 2.3.4, that the optimal point of the solution space belongs to  $\mathbb{D}_3^+ \cap \mathbb{D}^-(0)$  or  $\mathbb{D}_3^- \cap \mathbb{D}^-(0)$ , which correspond to two points that are denoted by  $(q^+, E^+)$  and  $(q^-, E^-)$ . It can be seen easily that  $E^{opt}$  is the smallest positive value between  $E^+$  and  $E^-$ . These two points are therefore defined as the solutions of the two systems

$$\left\{ \begin{array}{l} 1 + q^+ \cos [\pi \tilde{f}(x_1/L)] = E^+ \sin [\pi \tilde{f}] \\ \cos [\pi \tilde{f}] + q^+ \cos [\pi \tilde{f}(1 - x_1/L)] = -E^+ \sin [\pi \tilde{f}] \end{array} \right\}, \quad (56)$$

$$\left\{ \begin{array}{l} 1 + q^- \cos [\pi \tilde{f}(x_1/L)] = -E^- \sin [\pi \tilde{f}] \\ \cos [\pi \tilde{f}] + q^- \cos [\pi \tilde{f}(1 - x_1/L)] = -E^- \sin [\pi \tilde{f}] \end{array} \right\}. \quad (57)$$

The values of  $E^+$  and  $E^-$  are deduced:

$$E^+ = \frac{\sin [\pi \tilde{f}(x_1/L)]}{\cos [\pi \tilde{f}(1 - x_1/L)] + \cos [\pi \tilde{f}(x_1/L)]},$$

$$E^- = \frac{\sin [\pi \tilde{f}(x_1/L)]}{-\cos [\pi \tilde{f}(1 - x_1/L)] + \cos [\pi \tilde{f}(x_1/L)]}. \quad (58)$$

One can conclude that:

$$E^{opt}(x_1) = \sin [\pi \tilde{f}(x_1/L)] / \{ |\cos [\pi \tilde{f}(1 - x_1/L)]| + \cos [\pi \tilde{f}(x_1/L)] \}. \quad (59)$$

The derivative of  $E^{opt}(x_1)$  gives

$$\frac{dE^{opt}}{dx_1}(x_1) = \frac{\pi \tilde{f}}{L} \frac{1 + \text{sign} \{ \cos [\pi \tilde{f}(1 - x_1/L)] \} \cos [\pi \tilde{f}]}{\{ |\cos [\pi \tilde{f}(1 - x_1/L)]| + \cos [\pi \tilde{f}(x_1/L)] \}^2} \geq 0. \quad (60)$$

The inequality (60) proves that  $E^{opt}(x_1)$  increases from zero to  $1/|\sin(\pi \tilde{f})|$  when  $x_1$  varies from 0 to  $\lambda/4$ . In this space domain, there is no local minimum and the secondary source should be placed as close as possible to the left termination where the primary source is located.

3.1.2. *The distance  $x_1$  is superior to the quarter of the wavelength*

When the distance  $x_1$  is superior to the quarter of the wavelength the variations of  $E^{opt}$  with respect to  $x_1$  are more complicated. An example is presented in Figure 17 where the non-dimensional frequency is chosen to be equal to 3. The inequality (46) saying that  $1 \leq E^{opt} \leq 1/\sin(\pi \tilde{f})$  is verified again.

Local maxima of  $E^{opt}(x_1)$  are found for  $x_1$  equal to  $[(2n + 1)/2f]L$ , where  $n$  is an integer. For such locations the secondary acoustic path  $Z_1(x)$  is zero at the right side of the secondary source. The source cannot control the primary sound pressure in this area. At the right termination, for instance, the sound pressure is equal to  $(\rho_0 c_0 / S)j/\sin(\pi \tilde{f})$  for any secondary volume velocity. No active control is therefore achieved for these locations of the secondary source and  $E^{opt}$  is equal to  $1/|\sin(\pi \tilde{f})|$ .

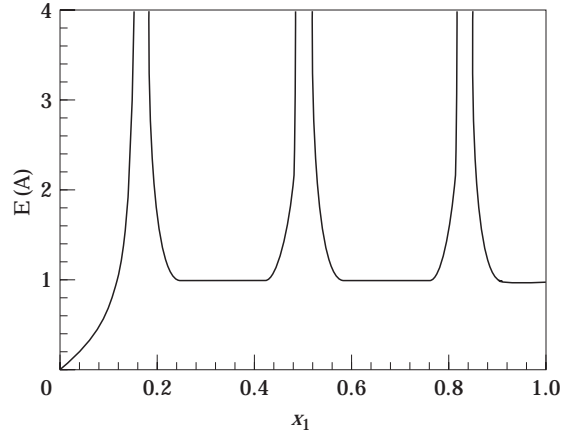


Figure 17. The maximal modulus of the non-dimensional sound pressure controlled with optimally located sensors against the source position  $x_1$  and  $\tilde{f}$  equal to 3.

When the distance  $x_1$  is superior to the quarter of the wavelength, one can show that the location of the secondary source  $x_1$  at the right termination is optimal. It has already been seen that  $E^{opt} \geq 1$ . With this location, it can be shown that  $E^{opt}$  is exactly equal to 1. The expression of the sound pressure field is indeed

$$p(x, q_1) = j \frac{\rho_0 c_0}{S} \left\{ \frac{\cos[\pi\tilde{f}(1-x/L)] + q_1 \cos(\pi\tilde{f}(x/L))}{\sin(\pi\tilde{f})} \right\}. \quad (61)$$

Suppose that the locations of two error sensors are the  $x_0$  and  $x_0 + \Delta x$  of the section 2.3. When  $\Delta x$  tends to zero, the optimal volume velocity again satisfies  $(\partial p / \partial x)(x_0, q_1^{opt}) = 0$ . With equation (61), this becomes

$$\sin[\pi\tilde{f}(1-x_0/L)] - q_1^{opt} \sin(\pi\tilde{f}(x_0/L)) = 0. \quad (62)$$

Since  $x_0$  corresponds to a sound pressure node of the secondary sound pressure field,  $\cos(\pi\tilde{f}(x_0/L)) = 0$  and the equation (62) can be simplified to

$$q_1^{opt} = -\cos(\pi\tilde{f}). \quad (63)$$

Hence

$$p(x, q_1^{opt}) = j \frac{\rho_0 c_0}{S} \left\{ \frac{\cos[\pi\tilde{f}(1-x/L)] - \cos(\pi\tilde{f}) \cos(\pi\tilde{f}(x/L))}{\sin(\pi\tilde{f})} \right\} = j \frac{\rho_0 c_0}{S} \sin(\pi\tilde{f}(x/L)). \quad (64)$$

Since  $E^{opt} = (S/\rho_0 c_0) \max_{x \in [0, L]} |\Im[p(x, q_1^{opt})]|$ ,

$$E^{opt} = \max_{x \in [0, L]} |\sin(\pi\tilde{f}(x/L))| \quad (65)$$

Since  $|\sin(\pi\tilde{f}(x_0/L))| = 1$ , one can conclude that  $E^{opt} = 1$  and that the location of the secondary source at the right termination is optimal.

### 3.2. SUFFICIENT NUMBER OF SECONDARY SOURCES

As the notation of a sufficient number of error sensors has been introduced previously, there is equally a sufficient number of secondary sources.

#### 3.2.1. A linear programming problem

One can now introduce a subset  $K$  of  $[0, L]$ . In numerical applications it is considered that  $K$  is a discrete subset containing  $N_0$  candidate locations for the secondary sources. The aim is to determine the sufficient number  $N$  of secondary sources and their locations. The sufficient number  $M$  of error sensors and their locations are found simultaneously.

The  $i$ th candidate location for a secondary source is denoted  $x_i$  and its corresponding real volume velocity is denoted  $q(x_i)$ .

Let  $Q_s$  denote a vector of  $\mathbf{R}^{N_0}$  that is equal to  $(q(x_1), \dots, q(x_i), \dots, q(x_{N_0}))$ . One then writes a new problem of minimization  $(\mathbb{A}_\epsilon)$ :

$$(\mathbb{A}_\epsilon) \min_{Q_s \in \mathbf{R}^{N_0}} J_\epsilon(Q_s) = \max_{x \in I} |\Im[p(x, Q_s)]| + \epsilon \sum_{i=1}^{N_0} |q(x_i)|, \quad (66)$$

where  $\epsilon$  is a small quantity. The second term of the cost function  $J_\epsilon$  is added in order to assure the uniqueness of the solution. The cost function  $J_\epsilon(Q_s)$  is strictly convex, whereas  $J(Q_s)$  is only convex. As is presented in Appendix 1, the simplex method actually solves the problem  $(\mathbb{A}_\epsilon)$  instead of the problem  $(\mathbb{A})$ .

The minimum  $Q_s^{opt}$  of the cost function  $J_\epsilon$  is a solution of the “minimax” problem. Among all the solutions of the “minimax” problem, the sum of the absolute values of the volume velocities is minimal with  $Q_s^{opt}$ .

An interesting property of this kind of problem (already used by Kirsch [14] for the optimal design of structural control systems) is that the solution is composed of a small number of non-zero variables.

As  $I$  has been introduced, one can define  $K'$ , a subset of  $K$ , as

$$K' = \{x \in K | q^{opt}(x) \neq 0\}. \quad (67)$$

The sufficient number  $N$  of secondary sources is equal to  $card(K')$  and their locations are defined by the subset  $K'$  itself. The problem  $(\mathbb{A}_\epsilon)$  can be written as a linear programming problem [15]. The sufficient numbers  $N$  and  $M$  of secondary sources and microphones and their respective locations are found by solving a unique linear programming problem.

#### 3.2.2. Application

The sets  $I$  and  $K$  are equal to  $[0, L]$  and  $[x_1, L]$  respectively.

When the distance  $x_1$  is superior to the quarter of the wavelength, it is found that a single source located at the right termination is optimal and sufficient for the “minimax” problem.

Now consider that  $x_1$  is inferior to the quarter of the wavelength. The sufficient numbers  $N$  and  $M$  are found to be equal to 2 and 3 respectively. The locations of secondary sources are  $x_1$  and  $L$ . The locations of the error sensors are 0,  $x_1$  and  $x_1 + \Delta x$ , where  $\Delta x$  is a small quantity representing the step of the mesh used for the numerical computation. Other locations are also optimal for the “minimax” problem but the sum of the absolute values of their volume velocities is larger.

Note again that

$$E^{opt}(x_1) = (S/\rho_0 c_0) \max_{x \in I} |\Im[p(x, Q_s^{opt})]|$$

and consider determining its variations with respect to  $x_1$ .

When  $\Delta x \rightarrow 0$ , the variables  $(q^{opt}(x_1), q^{opt}(L), E^{opt})$  are the solution of the system:

$$\begin{aligned} p(0, q^{opt}(x_1), q^{opt}(L)) &= E^{opt}, & p(x_1, q^{opt}(x_1), q^{opt}(L)) &= E^{opt}, \\ (\partial p / \partial x)(x_1^+, q^{opt}(x_1), q^{opt}(L)) &= 0, \end{aligned} \tag{68}$$

$$\left\{ \begin{aligned} \cos(\pi \tilde{f}) + q^{opt}(x_1) \cos[\pi \tilde{f}(1 - x_1/L)] + q^{opt}(L) &= E^{opt}, \\ \cos[\pi \tilde{f}(1 - x_1/L)] + q^{opt}(x_1) \cos[\pi \tilde{f}(1 - x_1/L)] \cos(\pi \tilde{f}(x_1/L)) \\ + q^{opt}(L) \cos(\pi \tilde{f}(x_1/L)) &= E^{opt}, \\ \sin[\pi \tilde{f}(1 - x_1/L)] + q^{opt}(x_1) \sin[\pi \tilde{f}(1 - x_1/L)] \cos(\pi \tilde{f}(x_1/L)) \\ - q^{opt}(L) \sin(\pi \tilde{f}(x_1/L)) &= 0. \end{aligned} \right. \tag{69}$$

The solution is

$$\begin{aligned} q^{opt}(x_1) &= -1, \\ q^{opt}(L) &= \operatorname{tg} \left( \frac{\pi \tilde{f} x_1}{2L} \right) \sin \left[ \pi \tilde{f} \left( 1 - \frac{x_1}{L} \right) \right], & E^{opt} &= \operatorname{tg} \left( \frac{\pi \tilde{f} x_1}{2L} \right). \end{aligned} \tag{70}$$

The results of the optimal placement of sources and sensors in the enclosure are summarized in Table 4. The obvious solution of the placement is the same location for the primary and the secondary source. This location is, in practical applications, often impossible. That is why a closest candidate point  $x_1$  has been considered for the placement of the secondary sources.

If  $x_1$  is inferior to the quarter of the wavelength of the primary excitation, two sources and three sensors are sufficient for active noise control. The particle volume velocity is cancelled on the right side of the point  $x_1$ .

If  $x_1$  is superior to the quarter of the wavelength of the primary excitation, a single source and two sensors are sufficient for active noise control. The particle volume velocity is cancelled at the point  $x_0$ , which corresponds to a node of the secondary sound pressure field.

### 3.3. MIXED PROGRAMMING

The method that is presented in the last section can be generalized by two means. First, bounds on the modulus of the volume velocities can be introduced. Second, the number  $N$  of active sources can be fixed inferior to the sufficient number of secondary sources.

In the presentation, one still considers  $Q_s$  in  $\mathbf{R}^{N_0}$ .

One introduces, therefore, a new problem of minimization  $(A_\varepsilon^N)$ :

$$(A_\varepsilon^N) \min_{Q_s \in \mathbf{R}^{N_0}} J_\varepsilon(Q_s) = \max_{x \in I} |\Im[p(x, Q_s)]| + \varepsilon \sum_{i=1}^{N_0} |q(x_i)|, \tag{71}$$

TABLE 4  
*Sufficient sources and sensors*

	$N$	$M$	Sources	Sensors	$E^{opt}(x_1)$
$x_1 \leq \lambda/4$	2	3	$x_1, L$	$0, x_1, x_1 + \Delta x$	$\operatorname{tg} \left( \frac{\pi \tilde{f} x_1}{2L} \right)$
$x_1 \geq \lambda/4$	1	2	$L$	$x_0, x_0 + \Delta x$	1

$$|q(x_i)| \leq A, \quad 1 \leq i \leq N_0, \quad \sum_{i=1}^{N_0} \chi(q(x_i)) \leq N. \quad (72)$$

The function  $\chi(q)$  is equal to zero if  $q$  is equal to zero and to one elsewhere. The absolute value of each secondary source is bounded by  $A$ .

### 3.3.1. Fixed charge problem

The problem of minimization can be written in another form:

$$\min_{Q_s, E} z = E + \varepsilon \sum_{i=1}^{N_0} |q(x_i)|, \quad (73)$$

$$\Im[p(x, Q_s)] \leq \frac{\rho_0 c_0}{S} E \quad \forall x \in I, \quad \Im[p(x, Q_s)] \geq -\frac{\rho_0 c_0}{S} E \quad \forall x \in I,$$

$$|q(x_i)| \leq A, \quad 1 \leq i \leq N_0, \quad \sum_{i=1}^{N_0} U_i \leq N, \quad U_i = \chi[q(x_i)]. \quad (74)$$

The variables  $U_i$  are integer, equal to zero or 1. The vector  $(U_1, \dots, U_i, \dots, U_{N_0})$  is noted  $U$ . The quantity  $\varepsilon$  is divided by  $\rho_0 c_0 / S$  compared with the expression (71).

The problem  $(\mathbb{A}_\varepsilon^N)$  is now similar to a problem of operational research called the fixed charge problem. Hirsch and Dantzig [16] formulated the problem as early as 1954. Hadley [17] demonstrated that the optimal solution of the fixed charge problem is a vertex of the convex space of solutions. The cost function can be computed at each vertex and the point realizing the minimum of the cost function is retained. Since the number of these vertices can be large, it is advantageous to use methods in which just a limited part of them is examined. Taha [18] presented some algorithms that have been specially developed for the fixed charge problem. He presented heuristic algorithms and exact algorithms. Among the latter ones, Hadley formulated the fixed charge problem as a problem of mixed programming with real and integer variables. The adaptation to the present problem is

$$\min_{Q_s, U, E} z = E + \varepsilon \sum_{i=1}^{N_0} |q(x_i)| + \varepsilon' \sum_{i=1}^{N_0} U_i, \quad (75)$$

$$\Im[p(x, Q_s)] \leq \frac{\rho_0 c_0}{S} E \quad \forall x \in I, \quad \Im[p(x, Q_s)] \geq -\frac{\rho_0 c_0}{S} E \quad \forall x \in I,$$

$$|q(x_i)| \leq AU_i, \quad 1 \leq i \leq N_0, \quad 0 \leq U_i \leq 1, \quad 1 \leq i \leq N_0,$$

$$U_i \text{ integer}, \quad 1 \leq i \leq N_0, \quad \sum_{i=1}^{N_0} U_i \leq N, \quad (76)$$

where  $\varepsilon'$  is a small quantity ( $\varepsilon' \ll \varepsilon$ ). The last term

$$\varepsilon' \sum_{i=1}^{N_0} U_i$$

assures the uniqueness of the solution.

### 3.3.2. Integer and mixed programming

Linear programming forms the basis for most of the development in integer or mixed programming. In integer programming, all of the variables are integer. In mixed programming, one part of the variables are integer and the rest is real. The fact that some variables are integer makes the problem more complicated. Taha [18] divided all the methods of integer programming into two groups: cutting-plane methods and branch-and-bound methods. In cutting methods, additional constraints cut off portions of the solution space so that no feasible points are ever excluded. In branch-and-bound methods, the non-promising feasible vectors are discarded without being tested. On the one hand, a large memory space of the computer is filled when the size of the tree becomes large. On the other hand, an approximated solution is available at an early stage of the computation. The bounds of the minimum are identified at each step. When the lower and the upper bounds are equal, an exact solution is determined. The bounds also provide information about the quality of the approximated solution that is found and updated during the computation.

### 3.3.3. Description of the algorithm

The branch-and-bound method of Land and Doig [19] is chosen here in order to solve the mixed programming problem (75), (76), the solution and minimum of which are denoted by  $(Q_s^{opt}, U^{opt}, E^{opt}, z^{opt})$ .

*Step 0.* By removing the constraint that compels the variables  $U_i$  to be integer, the problem (75), (76) is transformed into a linear programming problem that is solved by a simplex algorithm. The solution and minimum of this linear programming problem are denoted  $(Q_s^0, U^0, E^0, z^0)$ . The first lower bound  $B_-$  of  $z^{opt}$  is defined as

$$B_- = z^0. \quad (77)$$

One can now distinguish two cases.

A. If

$$\sum_{i=1}^{N_0} \chi(U_i^0) \leq N,$$

the algorithm is finished. The solution  $(Q_s^{opt}, U^{opt}, E^{opt})$  of the integer programming problem is equal to  $(Q_s^0, \chi(U^0), E^0)$ , where  $\chi(U^0) = (\chi(U_1^0), \dots, \chi(U_i^0), \dots, \chi(U_{N_0}^0))$ .

B. If

$$\sum_{i=1}^{N_0} \chi(U_i^0) > N,$$

the next step is prepared. An index for the first node is chosen. Choose  $i_0$  such that

$$U_{i_0}^0 = \max_{i \in \{1, \dots, N_0\}} \{U_i^0 | U_i^0 \neq 1\}. \quad (78)$$

$i_0$  is called the *branching index* of the first node. Each node is also endowed with a *root vector*  $S$  of dimension  $N_0$ , the components of which are equal to 0, 1 or 2. For the first node, the components  $S_i$  are all equal to 2. Each node is also endowed with a *cost*  $J$  that is a lower bound for all its child nodes. For the first node,  $J$  is equal to  $z^0$ .

*Step n.* Go to the node with the lowest cost (at step 1 there is a single node). This node has the branching index  $i_0$ , the root vector  $S$  and the cost  $J$  equal to  $B_-$ . Two child nodes are created now. One fixes  $S_{i_0} = 0$  for the daughter node and  $S_{i_0} = 1$  for the son node. A linear programming problem is associated to each child node. It again corresponds to the problem (75), (76), where the variable  $U_i$  is a real variable that is not constrained to be integer when  $S_i$  is equal to 2 and that is fixed to 0 or 1 in function of  $S_i$  elsewhere.

Let  $(\tilde{Q}_s, \tilde{U}, \tilde{E}, \tilde{z})$  denote the solution and the minimum of the linear programming problem associated to the son node (or daughter node).



TABLE 5  
Locations of sources with  $\tilde{f} = 0.5$

$N \setminus A$	1/4	1/3	1/2	1	10
1	1	1	1	1	1
2	1-2	1-2	1-2	1-21	1-21
3	1-2-3	1-2-3	1-2-21	—	—
4	1-2-3-21	1-2-3-21	—	—	—
5	1-2-3-4-21	—	—	—	—

A. Each child node again has a branching index  $i_0$  such that

$$\tilde{U}_{i_0} = \max_{i \in \{1, \dots, N_0\}} \{\tilde{U}_i \mid \tilde{U}_i \neq 1 \text{ and } S_i = 2\}. \quad (79)$$

B. Each child node has a cost  $J$  that is given by the minimum  $\tilde{z}$  of the associated linear programming problem. Among all the child nodes of the tree, the node with the lowest cost is determined. It is the next active node for the next step of branching. The cost  $J$  of this node is the new lower bound  $B_-$  of the problem. It is verified that the lower bound  $B_-$  increases at each step.

C. If

$$\sum_{i=1}^{N_0} \chi(\tilde{U}_i) \leq N$$

and if  $\tilde{z}$  is inferior to the present upper bound  $B_+$ , the upper bound is updated:

$$B_+ = \tilde{z}. \quad (80)$$

$(\tilde{Q}_s, \chi(\tilde{U}), \tilde{E})$  is a new approximated solution. It is verified that the upper bound  $B_+$  decreases during the computation.

D. If  $B_- = B_+$ , the algorithm is finished. The exact solution of the integer programming problem is  $(\tilde{Q}_s, \chi(\tilde{U}), \tilde{E})$ . If  $B_- < B_+$ , go to step  $n + 1$ .

### 3.3.4. Results of placement

Let the subsets  $I$  and  $K$  be equal to  $[0, L]$  and  $[x_1, L]$ . The distance  $x_1$  is chosen equal to  $L/2$ . The subsets are actually discretized with the step  $\Delta x$  equal to  $0.025 \times L$  corresponding to 41 points  $X_i$  for the sensors and 21 points  $x_i$  for the sources:

$$x_i = (L/2)\{1 + (i - 1)/20\}, \quad 1 \leq i \leq 21, \quad X_i = (L/2)(i - 1)/20, \quad 1 \leq i \leq 41. \quad (81)$$

Two non-dimensional frequencies are considered:  $\tilde{f}$  equal to 0.5 and 1.2, that correspond to a distance  $x_1$  inferior and superior, respectively, to one-quarter of the wavelength.

In Tables 5 and 6 are presented the optimal placement of sources at the two frequencies for different numbers  $N$  of sources and different bounds  $A$  on the volume velocities. Since  $q_p$  is chosen equal to 1, the bound  $A < 1$  constrains the modulus of the volume velocity

TABLE 6  
Locations of sources with  $\tilde{f} = 1.2$

$N \setminus A$	1/4	1/3	1/2	1	10
1	21	21	21	21	21
2	20-21	20-21	20-21	—	—
3	19-20-21	19-20-21	—	—	—
4	18-19-20-21	—	—	—	—
5	—	—	—	—	—

TABLE 7  
Sufficient number  $M$  of sensors with  $\tilde{f} = 0.5$

$N \setminus A$	1/4	1/3	1/2	1	10
1	1	1	1	2	2
2	1	1	2	3	3
3	2	2	3	—	—
4	2	3	—	—	—
5	2	—	—	—	—

of each secondary source to be inferior to the modulus of the volume velocity of the primary source.

When  $A$  is superior or equal to 1, the results of the placement of sources are identical to a problem with unconstrained volume velocities. When  $x_i$  is superior to one-quarter of the wavelength, the sufficient number of sources is equal to 1 and the secondary source is located at the right termination. When  $x_1$  is inferior to one-quarter of the wavelength, the sufficient number of sources is equal to 2 and the two secondary sources are located at the right termination and the point  $x_1$ . If a unique source is available, the optimal placement depends on the non-dimensional frequency  $\tilde{f}$  and on the point  $x_1$ . If  $E^{opt}(x_1)$  given by equation (59) is inferior to 1, the optimal placement is the point  $x_1$ . Otherwise, the right termination should be preferred. The optimal placement of a unique secondary source at the non-dimensional frequency  $\tilde{f} = 0.5$  is the point  $x_1$ .

When  $A$  is inferior to 1 and  $x_1$  is superior to one-quarter of the wavelength, the source at the right termination is split into several sources of smaller modulus of volume velocity. The sufficient number of sources is increased.

When  $A$  is inferior to 1 and  $x_1$  is inferior to one-quarter of the wavelength, the influence of the bounds on the placement of sources is more complicated. The solution of the unconstrained problem presented in section 3.2.2. gives  $q^{opt}(x_1) = -1$ . The source at the point  $x_1$  is therefore split into several sources when the bound  $A$  becomes inferior to 1.

### 3.3.5. Sufficient number of error sensors with bounded sources

For unbounded sources, it has been shown in section 2.2.3 that the sufficient number  $M$  (equal to  $card(I)$ ) of error sensors is equal to  $N + 1$ , where  $N$  is the number of secondary sources.

For bounded sources, the solution  $(Q_s^{opt}, E^{opt})$  belongs to  $\tilde{N}$  additional hyperplanes:

$$q_{i(\alpha)}^{opt} = \mp A, \quad \alpha \in \{1, \dots, \tilde{N}\}. \quad (82)$$

The integer number  $\tilde{N}$  is in  $[0, N]$ . The solution  $(Q_s^{opt}, E^{opt})$  belongs now to  $\tilde{N} + card(I)$  hyperplanes such that the equation (23) becomes

$$card(I) + \tilde{N} = N + 1. \quad (83)$$

Hence

$$1 \leq M \leq N + 1. \quad (84)$$

When the sources are bounded, the sufficient number  $M$  of error sensors decreases. The results for the two examples of the previous section are presented in Tables 7 and 8. The sufficient number  $M$  of error sensors is equal to  $N + 1$  only when the bound  $A$  is superior or equal to 1. In this case, the problem is identical to an unconstrained problem.

TABLE 8  
Sufficient number  $M$  of sensors with  $\tilde{f} = 1.2$

$N \setminus A$	1/4	1/3	1/2	1	10
1	1	1	1	2	2
2	1	1	2	—	—
3	1	2	—	—	—
4	2	—	—	—	—
5	—	—	—	—	—

### 3.3.6. Computational time

Let  $M_0$  and  $N_0$  denote the numbers of candidate locations for the sensors and sources (here equal to 41 and 21 respectively), and  $T$  the computational time required to solve the linear programming problem with  $M$  sensors and  $N$  sources. It has been found empirically that  $T \propto M^{1.5}N^{1.5}$ .

If  $n$  is the number of steps of the algorithm, the mixed programming problem requires that  $2n + 1$  linear programming problems with  $M_0$  sensors and  $N_0$  sources are solved. The computational time with the mixed programming is denoted by  $T_1$ . The number  $n$  is presented in Tables 9 and 10 for the two non-dimensional frequencies  $\tilde{f} = 0.5$  and  $\tilde{f} = 1.2$ . It is noticed that the problem often requires solving only one single linear programming problem (in all the cases when  $\tilde{f} = 1.2$ ):

$$T_1 \simeq (2n + 1) \times (M_0/M)^{1.5} (N_0/N)^{1.5} \times T. \quad (85)$$

One can now compare the computational time  $T_1$  with the computational time  $T_2$  if the whole set of  $C_{M_0}^M \times C_{N_0}^N$  linear programming problems with  $M$  sensors and  $N$  sources is solved:

$$T_2 = C_{M_0}^M \times C_{N_0}^N \times T. \quad (86)$$

The ratio  $T_2/T_1$  with  $\tilde{f} = 0.5$  is presented in Table 11. Mixed programming seems to be advantageous as soon as the number  $N$  of secondary sources exceeds one. It should be emphasized that the solution that is found is an exact solution of the “minimax” problem.

TABLE 9  
Number of steps  $n$  with  $\tilde{f} = 0.5$  (—, solution with a zero volume velocity)

$N \setminus A$	1/4	1/3	1/2	1	10
1	0	0	0	3	4
2	0	0	17	0	0
3	4	61	0	—	—
4	67	0	—	—	—
5	26	—	—	—	—

TABLE 10  
Number of steps  $n$  with  $\tilde{f} = 1.2$  (—, solution with a zero volume velocity)

$N \setminus A$	1/4	1/3	1/2	1	10
1	0	0	0	0	0
2	0	0	0	—	—
3	0	0	—	—	—
4	0	—	—	—	—
5	—	—	—	—	—

TABLE 11  
*Ratio  $T_2/T_1$  with  $\tilde{f} = 0.5$  (—, solution with a zero volume velocity)*

$N \setminus A$	1/4	1/3	1/2	1	10
1	0.03	0.03	0.03	0.3	0.2
2	1	1	2	$1 \times 10^3$	$1 \times 10^3$
3	70	5	$2 \times 10^4$	—	—
4	30	$1 \times 10^5$	—	—	—
5	$4 \times 10^2$	—	—	—	—

#### 4. CONCLUSIONS

An appropriate cost function called the “minimax” criterion better suits the strategy of selection in the placement of sensors and sources than the classic quadratic cost functions. This cost function is the largest squared pressure at a number of distributed points. Sufficient numbers of error sensors and secondary sources, their locations and the volume velocity of each secondary source are found simultaneously by solving a unique linear programming problem. An exact solution is determined in a short computational time.

The “minimax” criterion can be generalized by the introduction of bounds on the volume velocity of the secondary sources. Moreover, the number of sources can be fixed inferior to the “sufficient” number of sources. In this case a mixed programming problem is solved.

In an unidimensional enclosure with a primary source located at the left termination, the obvious solution consists of superposing the secondary source on the primary source. With the additional constraint that there is a minimal distance between the secondary source and the primary source, it is found that the problem of placement differs according to whether or not this minimal distance is inferior to one-quarter of the wavelength. When the minimal distance is inferior to one-quarter of the wavelength, the sufficient number of sources and sensors are two and three respectively. The first source is placed as close as possible to the primary source. The second source is located at the right termination. The particle volume velocity is cancelled on the right side of the first secondary source. When the minimal distance is superior to one-quarter of the wavelength, a single source at the right termination and two sensors are sufficient for active noise control. The particle volume velocity is cancelled on a node of the secondary sound pressure field.

#### REFERENCES

1. A. R. CURTIS 1988 *Ph.D. Thesis, University of Southampton*. The theory and application of quadratic minimization in the active reduction of sound and vibration.
2. E. BENZARIA and V. MARTIN 1994 *Journal of Sound and Vibration* **173**, 137–144. Secondary source locations in active noise control: selection or optimization?
3. K. H. BAEK and S. J. ELLIOTT 1995 *Journal of Sound and Vibration* **186**, 245–267. Natural algorithms for choosing source locations in active control systems.
4. S. POTTIE and D. BOTTELDOOREN 1996 in *Proceedings of Internoise 96*, 1001–1004. Optimal placement of secondary sources for active noise control using a genetic algorithm.
5. D. A. MANOLAS, T. GIALAMAS and D. T. TSAHALIS 1996 in *Proceedings of Internoise 96*, 1187–1191. A genetic algorithm for the simultaneous optimization of the sensor and actuator positions for an active noise and/or vibration control system.
6. J. K. KIM and J. G. IH 1995 in *Proceedings of Active 95*, 510–518. On the positioning of control sources for active noise control in 3-dimensional enclosed space.
7. E. BENZARIA and V. MARTIN 1995 in *Proceedings of Active 95*, 499–510. Constrained optimization of secondary source locations: multipolar arrangements.

8. F. ASANO, Y. SUZUKI, T. SONE and D. SWANSON 1995 in *Proceedings of Active 95*, 489–498. Optimization of control source location in active control systems.
8. B. NAYROLES, G. TOUZOT and P. VILLON 1994 *Journal of Sound and Vibration* **171**, 1–21. Using the diffuse approximation for optimizing the location of anti-sound sources.
10. T. C. YANG, C. H. TSENG and S. F. LING 1994 *Journal of the Acoustical Society of America* **95**, 3390–3399. Constrained optimization of active noise control systems in enclosures.
11. S. J. ELLIOTT, J. M. STOTHERS and P. A. NELSON 1987 *IEEE Transactions ASSP* **35**, 1423–1434. A multiple error L.M.S. algorithm and its application to the active control of sound and vibration.
12. G. B. DANTZIG 1963 *Linear Programming and Extensions*. Princeton, New Jersey: Princeton University Press.
13. P. A. NELSON and S. J. ELLIOTT 1992 *Active Control of Sound*. London: Academic Press.
14. U. KIRSCH 1991 *Engineering Optimization* **17**, 141–155. Optimal design of structural control systems.
15. P. SERGENT 1995 *Acta Acustica* **3**, 47–57. Optimal placement of sources for active noise control.
16. W. M. HIRSCH and G. B. DANTZIG 1968 *Naval Research Log Quarterly* **15**, 413–424. The fixed charge problem.
17. G. HADLEY 1964 *Non-linear and Dynamic Programming*. Reading, Massachusetts: Addison-Wesley.
18. H. A. TAHA 1975 *Integer Programming*. New York: Academic Press.
19. A. H. LAND and A. G. DOIG 1960 *Econometrica* **28**, 497–520. An automatic method for solving discrete programming problems.

## APPENDIX 1: TRANSFORMATION OF THE PROBLEM A

The linear problem is written first with an augmented cost function in order to assure the unicity of the solution. With a small quantity  $\varepsilon > 0$ , the cost function  $z$  becomes indeed strictly convex:

$$\min_{Q_s, E} z = E + \varepsilon \sum_{i=1}^N |q_i|, \quad (\text{A1})$$

$$\mathfrak{J}[p(x, Q_s)] \leq (\rho_0 c_0 / S)E \quad \forall x \in I, \quad \mathfrak{J}[p(x, Q_s)] \geq -(\rho_0 c_0 / S)E \quad \forall x \in I. \quad (\text{A2})$$

The positive and negative parts of the volume velocities  $q_i$  can then be introduced:  $\langle q_i \rangle_+ = \max(q_i, 0)$  and  $\langle q_i \rangle_- = \max(-q_i, 0)$ . The problem has now a new expression with  $2N + 1$  real positive variables:

$$\min_{Q_s^+, Q_s^-, E} z = E + \varepsilon \sum_{i=1}^N (q_i^+ + q_i^-), \quad (\text{A3})$$

$$\mathfrak{J}[p(x, Q_s^+ - Q_s^-)] \leq (\rho_0 c_0 / S)E \quad \forall x \in I,$$

$$\mathfrak{J}[p(x, Q_s^+ - Q_s^-)] \geq -(\rho_0 c_0 / S)E \quad \forall x \in I,$$

$$q_i^+ = \langle q_i \rangle_+, \quad q_i^- = \langle q_i \rangle_-. \quad (\text{A4})$$

Here  $Q_s^+$  and  $Q_s^-$  are the vectors of  $(\mathbf{R}^+)^N$  that are equal to  $(q_1^+, \dots, q_i^+, \dots, q_N^+)$  and  $(q_1^-, \dots, q_i^-, \dots, q_N^-)$  respectively.

By removing the last two equalities, the problem is written as a linear programming problem with a linear cost function and linear inequalities:

$$\min_{Q_s^+, Q_s^-, E} z = E + \varepsilon \sum_{i=1}^N (q_i^+ + q_i^-), \quad (\text{A5})$$

$$\mathfrak{J}[p(x, Q_s^+ - Q_s^-)] \leq (\rho_0 c_0 / S)E \quad \forall x \in I, \quad \mathfrak{J}[p(x, Q_s^+ - Q_s^-)] \geq -(\rho_0 c_0 / S)E \quad \forall x \in I. \quad (\text{A6})$$

One can now show that the solution  $(Q_s^{+opt}, Q_s^{-opt}, E^{opt})$  of this last problem satisfies, for all  $i$ ,  $q_i^{+opt} = \langle q_i^{opt} \rangle_+$  and  $q_i^{-opt} = \langle q_i^{opt} \rangle_-$  (i.e.,  $q_i^{+opt} = 0$  or  $q_i^{-opt} = 0$ ). If there exists an index  $i$  such that  $q_i^{+opt} \neq 0$  and  $q_i^{-opt} \neq 0$ , then  $(Q_s^{+opt}, Q_s^{-opt}, E^{opt})$  is not a solution of the problem of minimizing, because the cost function  $z$  can be reduced by the quantity  $2\varepsilon \min(q_i^{+opt}, q_i^{-opt})$  without changing the values of the inequalities. That proves that  $q_i^{+opt} = 0$  or  $q_i^{-opt} = 0$ . The equalities  $q_i^+ = \langle q_i \rangle_+$  and  $q_i^- = \langle q_i \rangle_-$  are therefore useless in the problem of minimization. The last problem, that is solved by the simplex algorithm, can therefore be used to determine the solution of the problem  $\mathbb{A}$ .

#### APPENDIX 2: DEMONSTRATION OF EQUATION (16)

If the set  $I$  is composed of a finite number of discrete points, one can show that (i) there exists a ball  $\mathbf{B}$  in  $\mathbf{R}^N$  of radius  $r_0$ , centered in  $Q_s^{opt}$  and of boundary  $\delta\mathbf{B}$  such that

$$Q_s^{opt} \in \mathbf{B}, \quad J(Q_s) = J'(Q_s) \quad \forall Q_s \in \mathbf{B}. \quad (\text{A7})$$

*Demonstration.* If (i) is false, for all  $r_0$  in  $\mathbf{R}^+$  there exists a unit vector  $Q_0$  in  $\mathbf{R}^N$  such that

$$\begin{aligned} \exists r \in ]0, r_0] \quad J(Q_s^{opt} + rQ_0) > J'(Q_s^{opt} + rQ_0), \\ \max_{x \in I'} |\mathfrak{J}[p(x, Q_s^{opt} + rQ_0)]| > \max_{x \in I'} |\mathfrak{J}[p(x, Q_s^{opt} + rQ_0)]|. \end{aligned} \quad (\text{A8})$$

When  $r_0 \rightarrow 0$ , equation (A8) becomes

$$\max_{x \in I'} |\mathfrak{J}[p(x, Q_s^{opt})]| \geq \max_{x \in I'} |\mathfrak{J}[p(x, Q_s^{opt})]|. \quad (\text{A9})$$

However, the definition of  $I'$  says that

$$\max_{x \in I'} |\mathfrak{J}[p(x, Q_s^{opt})]| < \max_{x \in I} |\mathfrak{J}[p(x, Q_s^{opt})]| \quad (\text{A10})$$

if  $I$  is composed of a finite number of points.

The contradiction between the inequalities (A9) and (A10) proves that (i) is true.

#### APPENDIX 3: DEMONSTRATION OF EQUATION (17)

One can show that the function  $J'(Q)$  is a convex function of  $\mathbf{R}^N$ .

*Demonstration.* Introduce three points  $Q_0$ ,  $Q_1$  and  $Q_2$  of  $\mathbf{R}^N$  such that

$$Q_0 = (1 - t)Q_1 + tQ_2, \quad t \in ]0, 1[. \quad (\text{A11})$$

There exists a point  $x'$  in  $I'$  such that

$$J'(Q_0) = |\mathfrak{J}[p(x', Q_0)]|. \quad (\text{A12})$$

Let  $F(Q)$  denote the function equal to  $|\mathfrak{J}[p(x', Q)]|$ . Since  $F(Q)$  is a convex function in  $\mathbf{R}^N$ ,

$$F(Q_0) \leq (1 - t)F(Q_1) + tF(Q_2). \quad (\text{A13})$$

Since  $F(Q) \leq J'(Q)$ ,

$$J'(Q_0) \leq (1 - t)J'(Q_1) + tJ'(Q_2). \quad (\text{A14})$$

The function  $J'(Q)$  is therefore a convex function in  $\mathbf{R}^N$ .